Journal of Power Sources 397 (2018) 231–239

Contents lists available at ScienceDirect

Journal of Power Sources

journal homepage: www.elsevier.com/locate/jpowsour

Highly conductive $CrNb_{11}O_{29}$ nanorods for use in high-energy, safe, fast-charging and stable lithium-ion batteries

Qingfeng Fu[a,b,c], Xin Liu[a,b,c], Jingrong Hou[a,b,c], Yiran Pu[a,b,c], Chunfu Lin[a,b,c,*], Liang Yang[c], Xiangzhen Zhu[a,b,c], Lei Hu[a,b,c], Shiwei Lin[b,c], Lijie Luo[b,c], Yongjun Chen[b,c]

[a] Key Laboratory of Advanced Materials of Tropical Island Resources (Hainan University), Ministry of Education, Haikou 570228, China
[b] State Key Laboratory of Marine Resource Utilization in South China Sea, Haikou 570228, China
[c] College of Materials and Chemical Engineering, Hainan University, Haikou 570228, China

HIGHLIGHTS

- $CrNb_{11}O_{29}$ is explored as a new intercalating anode material for Li^+-ion batteries.
- $CrNb_{11}O_{29}$ shows a large electronic conductivity and Li^+-ion diffusion coefficient.
- $CrNb_{11}O_{29}$ nanorods are facilely synthesized based on a novel hydrothermal method.
- $CrNb_{11}O_{29}$ nanorods show significant pseudocapacitive behavior during the reaction.
- $CrNb_{11}O_{29}$ nanorods show a high capacity, safety, rate capability and cyclability.

GRAPHICAL ABSTRACT

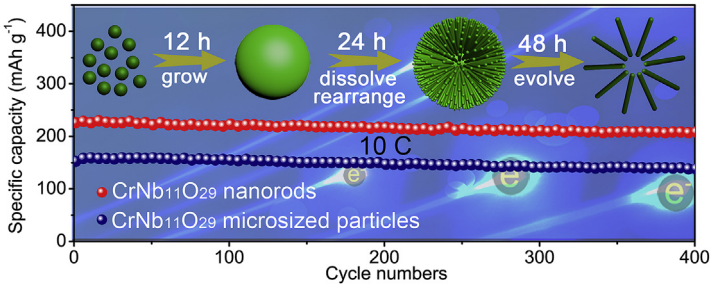

ARTICLE INFO

Keywords:
$CrNb_{11}O_{29}$
Electrochemical performance
Lithium-ion battery
Nanorod
Negative electrode

ABSTRACT

$Ti_2Nb_{2x}O_{4+5x}$ compounds are very popular negative-electrode materials for lithium-ion batteries due to their high specific capacities, safe operating potentials and high cycling stability. Nevertheless, their poor electronic conductivities and insufficient Li^+ diffusion coefficients limit the rate capabilities. Herein, we explore highly conductive $CrNb_{11}O_{29}$ with a high theoretical capacity (401 mAh g^{-1}) and an open Wadsley–Roth shear structure as a new intercalating negative-electrode material having the same advantages of $Ti_2Nb_{2x}O_{4+5x}$ but a high rate capability. $CrNb_{11}O_{29}$ nanorods ($CrNb_{11}O_{29}$-R) with lengths of 500–1000 nm and very small diameters of 30–50 nm are prepared based on a novel hydrothermal method. Due to the free electrons in Cr-3d orbitals and the large ionic radius of Cr^{3+}, $CrNb_{11}O_{29}$ exhibits a high electronic conductivity and large Li^+ diffusion coefficients, respectively. *In-situ* X-ray diffraction analyses confirm its high structural stability. These conductivity, structural and architectural advantages in $CrNb_{11}O_{29}$-R lead to its significant pseudocapacitive contribution (82.0% at 1.1 mV s^{-1}), prominent rate capability (high reversible capacities of 343 mAh g^{-1} at 0.1C and 228 mAh g^{-1} at 10C), and outstanding cycling stability (only 8.9% capacity loss at 10C over 400 cycles).

* Corresponding author. Key Laboratory of Advanced Materials of Tropical Island Resources (Hainan University), Ministry of Education, Haikou 570228, China.
E-mail address: linchunfu@hainu.edu.cn (C. Lin).

https://doi.org/10.1016/j.jpowsour.2018.07.020
Received 26 April 2018; Received in revised form 8 June 2018; Accepted 4 July 2018

1. Introduction

Due to the merits of the high energy density, long storage life, long cycling life, low self-discharge, low environmental impact, and absence of memory effects, lithium-ion batteries (LIBs) are extremely popular as the power sources for portable electronic devices. In recent years, the LIBs for large scale energy-storage systems, such as electric vehicles (EVs), have aroused extensive attention [1,2]. At present, the main limitation for the future industrial development of EVs is the insufficient performance of LIBs, partly resulting from the lack of high-performance negative-electrode materials [3,4]. Graphite is the most popular negative-electrode material for commercial LIBs owing to its low processing cost, high specific capacity (theoretically 372 mAh g^{-1}), and environmental benignity. Nevertheless, it suffers from three drawbacks: (i) a serious safety issue arising from the generation of lithium dendrites at its extremely low operating potential (< 0.2 V); (ii) a poor rate capability arising from its insufficient Li^+ diffusivity and the generation of thick solid electrolyte interphase (SEI) layers at < 1.0 V; and (iii) disappointing cycling stability caused by its large volume variation ($\sim 9\%$) during full lithiation and delithiation [5]. Thus, to meet the large-scale applications of LIBs, it is of great importance to explore new negative-electrode materials with desirable properties, including high safety, capacities, rate capabilities and cycling stability [6].

Recently, $Ti_2Nb_{2x}O_{4+5x}$ ($x = 2$, 5 and 24) compounds have emerged as very promising negative-electrode materials due to their safe operating potentials, high theoretical capacities, high cycling stability and significant intercalation pseudocapacitive behavior [7–29]. $Ti_2Nb_{10}O_{29}$ ($x = 5$) is taken as an example. The Nb^{3+}/Nb^{4+}, Nb^{4+}/Nb^{5+} and Ti^{3+}/Ti^{4+} redox couples in $Ti_2Nb_{10}O_{29}$ are active in a safe potential window of 1.0–2.0 V, inhibiting the generation of lithium dendrites and SEI layers [16]. $Ti_2Nb_{10}O_{29}$ has a high theoretical capacity of 396 mAh g^{-1} calculated from its 22-electron transfer *per* $Ti_2Nb_{10}O_{29}$ formula unit. This theoretical capacity is even higher than that of graphite. $Ti_2Nb_{10}O_{29}$ shows a Wadsley–Roth shear structure, which is built by $3 \times 4 \times \infty$ octahedron-blocks sharing corners and/or edges [16]. The edge sharing significantly stabilizes the crystal structure. The high structural stability together with the intercalating characteristic of $Ti_2Nb_{10}O_{29}$ results in its high cycling stability. Furthermore, since $Ti_2Nb_{10}O_{29}$ has an open Wadsley–Roth shear structure, it presents an intrinsic intercalation pseudocapacitive feature [26–28,30]. Intercalation pseudocapacitance often occurs when ions intercalate into the tunnels or layers of a redox-active material accompanied by a faradaic charge-transfer with no crystallographic phase change. It benefits the rate capability because it is not controlled by solid-state diffusion. Nevertheless, $Ti_2Nb_{10}O_{29}$ is an insulator due to the empty 3d (4d) orbitals in the Ti^{4+} (Nb^{5+}) ions with the highest oxidation state. The resulting low electronic conductivity together with the insufficient Li^+ diffusion coefficient in $Ti_2Nb_{10}O_{29}$ leads to its poor rate capability and significantly limits its practical applications in LIBs [22]. Hence, it is highly desirable to develop new niobium-based negative-electrode materials with the same advantages of $Ti_2Nb_{2x}O_{4+5x}$ but high rate capabilities for better Li^+ storage.

Here, we explore highly conductive $CrNb_{11}O_{29}$ as a better negative-electrode material than insulating $Ti_2Nb_{10}O_{29}$. Pure $CrNb_{11}O_{29}$ micro-sized particles ($CrNb_{11}O_{29}$-P) are prepared by a traditional solid-state reaction at a high sintering temperature of 1250 °C in a N_2 atmosphere (Fig. 1). Due to the multiple redox couples of Nb^{3+}/Nb^{4+}, Nb^{4+}/Nb^{5+} and Cr^{2+}/Cr^{3+}, there is theoretically 23-electron transfer *per* $CrNb_{11}O_{29}$ formula unit. Thus, the theoretical capacity of $CrNb_{11}O_{29}$ can be calculated to be 401 mAh g^{-1}, higher than that of $Ti_2Nb_{10}O_{29}$. Cr^{3+} ($t_{2g}^3 e_g^0$) is a conductive ion with three free electrons in its 3d orbitals [31], leading to the high electronic conductivity of $CrNb_{11}O_{29}$. The ionic radii of Cr^{3+} (0.615 Å in octahedral sites) and Nb^{5+} (0.64 Å) are larger than that of Ti^{4+} (0.605 Å) [32], resulting in an increase of the unit-cell volume, which benefits the Li^+ diffusion. Therefore, $CrNb_{11}O_{29}$ is expected to be a negative-electrode material with all the advantages of $Ti_2Nb_{10}O_{29}$ but a higher reversible capacity and rate capability. In order to further enhance the electrochemical performance of $CrNb_{11}O_{29}$, $CrNb_{11}O_{29}$ nanorods ($CrNb_{11}O_{29}$-R) are innovatively synthesized through a simple hydrothermal route and subsequent low-temperature sintering at 850 °C in N_2 (Fig. 1). The nanorod architecture can shorten the Li^+/electron transportation lengths in the nanorods, facilitate the electron transportation along the nanorods, and enlarge the electrolyte/electrode interface area [14,33]. Consequently, $CrNb_{11}O_{29}$-R owns comprehensively good electrochemical performance, including a high reversible capacity, safety, initial Coulombic efficiency, cycling stability and rate capability.

2. Experimental

2.1. Material preparations

$CrNb_{11}O_{29}$-P with microsized particles was synthesized by a typical solid-state reaction method (Fig. 1). Stoichiometric amounts of Nb_2O_5 (Aladdin, 99.5%) and Cr_2O_3 (Aladdin, 99.99%) powders (Nb:Cr = 11:1 in mol/mol) were mixed together. The mixture was then ball-milled by a high-energy ball milling machine with zirconia balls (SPEX 8000 M) for 60 min, and finally sintered at 1250 °C for 4 h in a N_2 atmosphere with a heating rate of 10 °C min^{-1}.

$CrNb_{11}O_{29}$-R with nanorods was synthesized by a novel hydrothermal method and subsequent low-temperature sintering (Fig. 1). $NbCl_5$ (Aladdin, 99.5%) and $Cr(NO_3)_3{\cdot}9H_2O$ (Aladdin, 99.9%) were employed as Nb and Cr precursors, respectively. 0.011 mol $NbCl_5$ and 0.001 mol $Cr(NO_3)_3{\cdot}9H_2O$ were dissolved in a 50 mL solution of 3.0 M hydrochloric acid (HCl). After gentle stirring for 0.5 h, the resulting solution was devolved to an autoclave whose inner volume was 100 mL. The autoclave was maintained in an oven at 200 °C for 48 h. The obtained precipitates were centrifuged, washed with ethyl alcohol for five times, and then dried at 80 °C in an oven overnight. The fully dried powders were sintered at 850 °C for 4 h in N_2 with a heating rate of 1 °C min^{-1}.

2.2. Material characterizations and simulations

XRD experiments were implemented on an X-ray diffractometer (Brucker D8) to characterize the crystal structures of $CrNb_{11}O_{29}$-P and $CrNb_{11}O_{29}$-R. A Rietveld refinement of the XRD spectrum of $CrNb_{11}O_{29}$-P was conducted with the general structure analysis system (GSAS) suite of programs [34,35]. An XPS equipment (Thermo Escalab 250Xi) was adopted to define the chemical valences of the cations. High resolution TEM (HRTEM, FEI Tecnai, G2F20) and field emission SEM (FESEM, Hitachi S-4800) equipments were used to reveal the morphology differences between $CrNb_{11}O_{29}$-P and $CrNb_{11}O_{29}$-R. Nitrogen physisorption was performed on a surface area analysis equipment (Micromeritics ASAP 2020) to examine the specific surface areas of the two $CrNb_{11}O_{29}$ samples. The electronic conductivity of $CrNb_{11}O_{29}$ was measured by two-probe direct current tests of disc-shaped Au/$CrNb_{11}O_{29}$/Au blocking cells, which were fabricated according to a procedure previously reported [22,36]. An electrochemical workstation (Zahner Zennium, Kronach) was employed to implement the electronic-conductivity tests. *In-situ* XRD tests were performed on an *in-situ* cell with an X-ray-transparent beryllium window (Fig. S1). The first-principles calculations of $CrNb_{11}O_{29}$ were carried on by employing a method previously developed [19,22,37–41]. The calculation model was simulated in a 41-ion primary cell.

2.3. Electrochemical tests

The electrochemical performance of $CrNb_{11}O_{29}$-P and $CrNb_{11}O_{29}$-R was analyzed by means of CR2016-type coin cells containing lithium foils, microporous polypropylene films (Celgard 2325), electrolyte and